



## REINFORCED OF PIERS OF A BRIDGE TYPE USING FRAGILITY CURVES

M. C. Gómez Soberón <sup>(1)</sup>, C. Cruz Martínez <sup>(2)</sup>,

<sup>(1)</sup> Professor-Researcher, Universidad Autónoma Metropolitana, UAM, Azcapotzalco; México. [cgomez@correo.azc.uam.mx](mailto:cgomez@correo.azc.uam.mx)

<sup>(2)</sup> Postgraduated Student, Universidad Autónoma Metropolitana, UAM, Azcapotzalco; México. [cesar\\_cruz\\_mtz@hotmail.com](mailto:cesar_cruz_mtz@hotmail.com)

### **Abstract**

Most of the existing bridges in Mexico were built 30 years ago or more (similar to that of other countries), so maintenance and reinforced programs are necessary to rehabilitate old structures before earthquakes take place. To define the best rehabilitation technique depends on the bridge type, damage degree of the elements, earthquake characteristics and economic aspects. Most of the time, the reinforcement condition is decided for each special case.

This paper presents a reinforcement procedure to define the best rehabilitation technique of piers of a bridge type, with single wall pier by bent. The best rehabilitation technique is defined in function of probabilistic aspects, using fragility curves. To do this, mechanical properties of the piers material are considered as random variables with probabilistic distribution function, mean and variation coefficient are considered from the available literature. Also, earthquake load is random considering four seismic scenarios and artificial records. For the original structures the fragility curves were defined by means of a Monte Carlo simulation for the four seismic scenarios. Damage is represented by the local and global Park indices. Then, light, moderate and severe damage were simulated in most earthquake susceptible pier. Damage is simulated considering degradation of pier section in function of experimental test reported in literature. For example, light damage, almost 10% of degradation, is represented by the same original section without concrete cover, because it was observed in experimental test of piers elements that the concrete cover is lost in a few cycles. For damaged structures fragility curves were again determined. Degraded bridges were reinforced using conventional techniques, specifically steel, concrete and fiber jackets, only for the damaged piers. The dimensions of the jackets were first selected considering that the fragility curves of these structures were similar to the ones of the original bridges. But it was not always possible; for example the minimum thick recommended produces a null damage index in the most of the Monte Carlo simulation of elements with light damage. Fragility curves of original, damaged and reinforced bridges were compared. Through this comparison, the best option to reinforce the bridge piers is selected, and some practical recommendations were expressed.

*Keywords: bridge reinforcing; fragility curves; piers jacketing*



## 1. Introduction

Bridges are some of the most vulnerable elements of the lifeline transportation networks. Failure in bridges could produce loss of human lives and important direct and indirect economic loss, principally for the rehabilitation or reposition of the structure and for the lack of its function.

Fragility curves are decision tools used to define maintenance and rehabilitation programs, because of this, more vulnerable elements or systems are characterized to define the optimal rehabilitation procedure of the damaged structure. Fragility curves are obtained in several procedures; some of the most used in recent years are the probabilistic analytical methods. Choi *et al.*, (2004) define fragility curves of existing straight bridges. The stochastic methods with Monte Carlo simulation and artificial records are used to define fragility functions, as by Nasseradi *et al.*, (2009). Fragility curves were defined by Liao y Loh (2004) for bridges in Taiwan, by analyzing reported damages. Karim and Yamazaki (2000) define fragility curves for typical bridges in Japan through a damage indices formulation. Nielson and DesRoches (2007) used limited functions, like the lognormal distribution, to characterize demand and capacity of bridge elements and, then, to obtain fragility curves for bridges in the United States. Zhang *et al.*, (2008) define fragility curves for several bridge configurations, including girder-to-pier connection, abutment type or the existence or not of isolation elements, by using stochastic evaluations. In addition, Mackie and Nielson (2009) evaluated the influence of different uncertainties in the fragility curves evaluation by applying probabilistic tools. Padgett and DesRoches (2008) used fragility curves as tools to find out the best rehabilitation technique of reinforced bridges. Olmos *et al.*, (2014) analyzed, by probabilistic estimations, the seismic response of rehabilitated bridges with steel jackets in piers. Mohsebni (2012) studied the seismic vulnerability of highway and railway bridges to different loads, evaluating steel truss bridges, and multispan curved highway bridges through its fragility curves. Other papers indicated that fragility curves were utilized as useful decision tools for maintenance and rehabilitation programs. However, in Mexico just a recent work has been dedicated to evaluate fragility curves for typical highway bridges, to formalize a reliable database.

In other aspects, designers do not have complete information to decide which is the best rehabilitation technique for bridge piers; since some authors think that the best rehabilitation technique depends on the element damage state and the structure configuration. Then, in this paper, fragility curves of elements and systems of a common bridge configuration in Mexico were evaluated. Starting from these curves, some damage levels were assumed in the most vulnerable element and fragility curves were defined again. Finally, for every damaged bridge, steel, concrete and fiber jackets were used to rehabilitate bridge piers and fragility curves were evaluated. The comparison of all fragility curves were used to reach some recommendations.

## 2. Motin de Oro bridge

The typical highway bridge studied was the Motin de Oro structure. This bridge is a continuous RC structure, almost symmetrical, with four spans of 25.15 m, 29.65 m, 29.90 m and 25.15 m, with a total length of 109.85 m. The bridge has three-single concrete bent piers of 4.11m, 4.26 m and 4.46 m, with a wall-box transverse section. The superstructure is a unicellular prestressed box girder of 10 m by 1.8 m of transversal and vertical dimensions, based on elastomeric bearings. In Figure 1 it is observed a photograph of the structure, the general dimensions of the girder and a scheme in elevation of the bridge.

Motín de Oro bridge was repaired in 1994 by using external and longitudinal cables, as shown in the photograph of figure 1. However, the analysis developed in this work is related to the substructure condition and repair, so fragility curves developed in this paper were evaluated for the original condition.

Motin de Oro bridge was selected because it was used in other studies, we have the general dimensions of structure and elements, and principally, because an experimental campaign was carried out to define the main dynamic characteristics of the structure. From the experimental campaign, it was defined that the first two



periods of this structure, without external and longitudinal cables in superstructure systems, are of 0.342 s for longitudinal direction and 0.276 s for transversal direction.

Motin de Oro bridge was modeled in SAP 2000 and Ruaumoko 3D codes. Structure was modeled in SAP 2000 (2008) because this code offers more tools, like the ones to define bearings elements, while we use Ruaumoko 3D (Car, 2004) to perform the nonlinear analysis. The SAP model was calibrated with experimental campaign. SAP 2000 and Ruaumoko 3D models can be observed in Figure 2. In both codes, piers were assumed as embedded and bearings are considered as elastic links. For the nonlinear model, the interaction and moment-curvature diagrams for piers elements are needed, because the superstructure systems was assumed elastic as was reported in many works. These curves were defined considering uncertainty on the mechanical properties of materials, as it was commented later. In addition, for nonlinear model, Takeda was used to define constitutive laws of pier elements. Piers ductility capacity was evaluated by applying the Prietsley and Park (1989) expression, define by:

$$\mu = \left[ \frac{3\phi_{\max}}{\phi_y - 1} \right] \left[ \frac{L_p}{L} \right] \left[ \frac{1 - 0.5L_p}{L} \right] \quad (1)$$

where  $L_p$  is the plastic hinge length,  $L$  is the distance between the column base and the center of mass of the superstructure,  $\phi_y$  and  $\phi_{\max}$  are, respectively, the yield and maximum curvature at the column base. Eq.1 assumed that the horizontal earthquake load acts in the system center of mass.

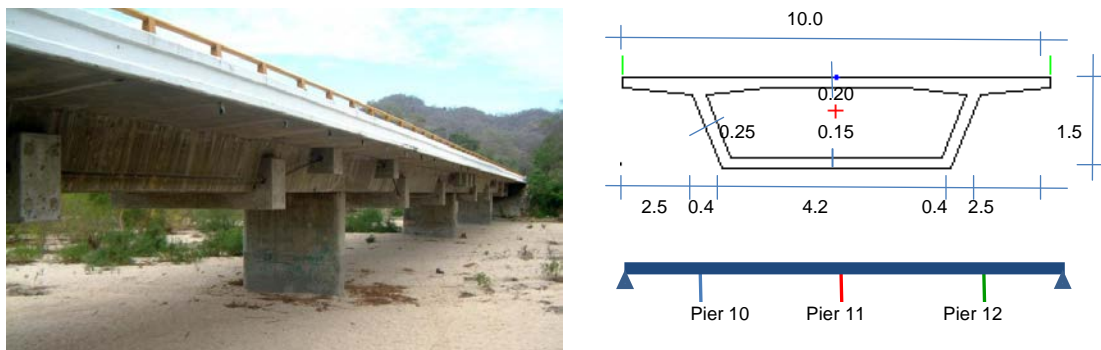


Fig. 1 – Motin de Oro bridge, photograph, transversal section of girder and elevation scheme

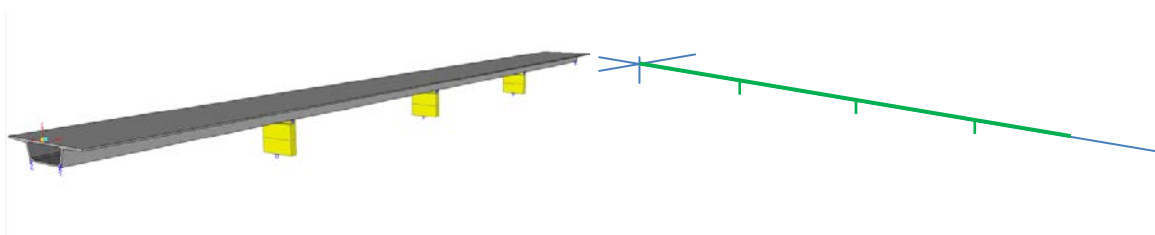


Fig. 2 – Sap 2000 (left) and Ruaumoko 3D (right) models for the study bridge



## 2.1 Uncertainty consideration

The external seismic load uncertainty was considering by four seismic scenarios and by the use of artificial accelerograms. The seismic scenarios were defined analyzing the registered accelerograms in stations near the bridge location, in the Pacific Coast of Mexico (one of the most hazardous seismic zones of the country). Then, four seismic scenarios were defined: 1) January 11th, 1997, with  $PGA=396 \text{ cm/s}^2$ ; 2) October 12th, 1995, with a  $PGA=227 \text{ cm/s}^2$ ; 3) April 30th, 1986, with  $PGA=69.2 \text{ cm/s}^2$ ; and 4) September 19th, 1985, with  $PGA=140 \text{ cm/s}^2$ , the record with larger duration of the intense phase. Accelerograms and elastic spectra of the four seismic scenarios, for a 5% of critical damping and for the horizontal direction with greater values, are shown in Figure 3. As it is observed, the fundamental periods of the accelerograms are less than 0.5 s. Therefore, the two fundamental periods of the bridge are in the zone of larger amplitude of the spectrum. Based on the signals of Figure 3, artificial records were generated by seeking similar velocity spectrums and keeping in mind that the accelerogram is formed by the sum of an infinite number of sine functions, with random phase angle between 0 and  $2\pi$ .

The uncertainty of mechanical properties of the elements materials was considered by the probabilistic properties of the variables show in Table 1. The assumed probabilistic distributions of these variables and their means and variation coefficient, taken from the available literature, are shown in this table. Dimension variables were assumed as deterministic, because their dispersions are minimal.

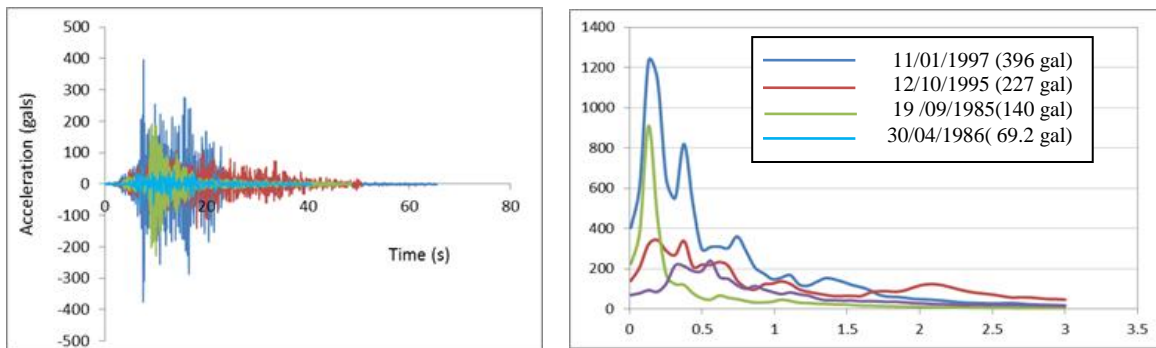


Fig. 3 – Accelerograms and elastic spectrum for the mayor horizontal component of the four seismic scenarios

Table 1 – Probabilistic models of the mechanical properties

Variable	Description	Mean	CV	Distribution
$f'_c$ (kPa)	Concrete compressive strength	28890	0.064	Normal
$E_c$ (kPa)	Concrete elastic modulus	22000000	0.077	Lognormal
$w_c$ (kN/m <sup>3</sup> )	Concrete specific weight	24	0.040	Normal
$f_y$ (kPa)	Steel yield stress	412020	0.064	Normal
$f_u$ (kPa)	Steel ultimate stress	618030	0.064	Normal
$E_s$ (kPa)	Steel elastic module	210000000	0.080	Lognormal
$w_s$ (kN/m <sup>3</sup> )	Steel specific weight	77	0.010	Normal



## 2.2 Nonlinear analyses of the original bridge

Considering uncertainty in seismic load and mechanical properties of materials (Fig.3 and Table 1), Monte Carlo simulation technique was used to define fragility curves. For this, 300 variations of the nonlinear analyses by each seismic scenario were used to define local and global damage indices. The number of variations analyses was defined by considering that the mean value of the results is nearly constant when it is close to 300.

The damage indices formulation used in this work was the one proposed by Park and Ang. (1985), because it is simple and it has an exhaustive calibration with experimental test. Local, for elements, and global, for a system, damage indices proposed by Park *et al.* are expressed as

$$ID = \frac{\delta_m}{\delta_u} + \frac{\beta}{F_y \delta_u} \int dE \quad (2)$$

$$ID_G = \frac{\sum_i ID_i^2}{\sum_i ID_i} \quad (3)$$

where  $\delta_m$  and  $\delta_u$  are, respectively, the maximum and ultimate strain of the element subjected to monotonic load,  $\beta$  represents the strength loss ( $\beta=0.15$ ),  $E$  is the hysteretic dissipated energy,  $F_y$  is the yield load and  $ID_G$  and  $ID$  are the global and local indices. In Eq. 3 it is observed that the global damage index is a weight average of the damage indices of the elements, so it is not always the best representation of the damage of the structure.

Through the nonlinear analyses local and global damage indices were defined for each pier and the entire bridge, and for the 300 variations and four seismic scenarios (in Gómez and Soria, 2014, the fragility curves of the bridge for all seismic scenarios could be observed, although it did not consider the probabilistic variation of the capacity of ductility). For each seismic scenario, 300 damage indices for every element were adjusted to theoretical probabilistic distribution functions, defined as the fragility curves. In Figure 4, fragility curves for piers and the entire Motín de Oro bridge are presented for the first seismic scenario, the one with largest PGA; results for other seismic scenarios were not presented because the limited space. In this figure, it is observed that the element 12, the far right pier of models of Figure 1, is the element more susceptible to seismic load of the first seismic scenario. In Figure 1, it is presented the position of each pier according to the color code used for the fragility curves. For example, the probability of a moderate damage,  $P[Damage > 0.2/SS1]$ , are of 0.26, 0.50 and 0.75 for piers 10, 11 and 12, respectively, being SS1 the first seismic scenario. The global damage of the structure is obtained by using Equation 3. As observed in Figure 4, the probability of a global damage larger than 0.2 (moderate damage) is 0.45.

## 2.3 Nonlinear analyses of the damaged bridge

As it was commented, the most vulnerable element for the Motín de Oro bridge is the pier 12, the one with the largest probability to suffer a greater certain damage level for the first seismic scenario. In this work, it is assumed that this pier is the one that sustains damage before than the other piers. As it is difficult to assign a specific damage percentage, three qualitative damage levels were used to represent the pier degradation: light, moderate and severe damage. The condition of a RC damaged element for the three damage levels was assumed as a function of experimental results. Specifically, the results of Posada (1994) were studied, with experimental analyses of RC columns up to the collapse.

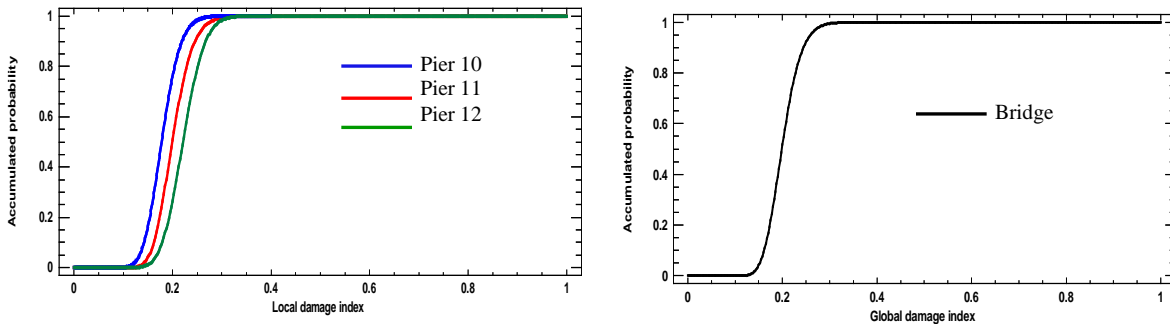


Fig. 4– Fragility curves for piers (left) and the bridge (right) for the first seismic scenario

For a light damage of the pier 12, almost a 10% of degradation is considered for the case when the concrete cover is lost and the resistance of the element is proportionated by the reinforcing steel and the central concrete confined by stirrups. When the concrete cover is removed, it is assumed that the concrete has been cracked due to weathering agents, allowing the reinforcing steel corrosion. For moderate and severe damage, almost 20% and 40% of degradation, some damage is considered in the longitudinal steel and core concrete materials, so that the areas of these elements were degraded in relation to these percentages. In Figure 5, degradation schemes for each level of damage on damaged piers are shown.

For the damaged element, new moment-curvature and interaction diagrams are needed, considering the properties of the degraded sections and the random nature of seismic load and mechanical parameters of Table 1. Then, again 300 variations for the Monte Carlo simulation were developed and distribution functions were adjusted.

Fragility curves for bridges with a damaged pier are presented in Figures 6 to 8 for light, moderate and severe damage, respectively. These figures show the fragility curves for piers on the left and for the entire bridge on the right. As observed in Figure 6, when light damage is assumed for pier 12, the fragility curves are similar to the ones of Figure 4. For example,  $P[Damage > 0.2/SS1]$  are of 0.4, 0.7, 0.1 and 0.22 for piers 10, 11 and 12, and for the bridge, respectively. Then, probability of certain damage is larger for piers 10 and 11, but lower for pier 12, maybe because the difference of the adjusted theoretical function. In Figure 7, when a moderate damage is simulated for pier 12, the fragility curves for not damaged piers (10 and 11) are similar to the not damage option, but for pier 12 the probabilities are larger. For example,  $P[Damage > 0.2/SS1]$  are of 0.25, 0.5, 0.98 and 0.9, for piers 10, 11, and 12 and for the bridge, respectively. Although the probabilities of damage of piers 10 and 11 are similar, the greater probability of damage of pier 12 produces an increase of the bridge damage probability. For a single pier bent structure as the Motín de Oro bridge, the failure of a pier is the failure of the system. For a severe damage of pier 12 (Figure 8), similar tendencies are obtained. In this case, the probability to suffer moderate damage for pier 12 is a certain event and the probability of moderate damage in bridge is 0.95.

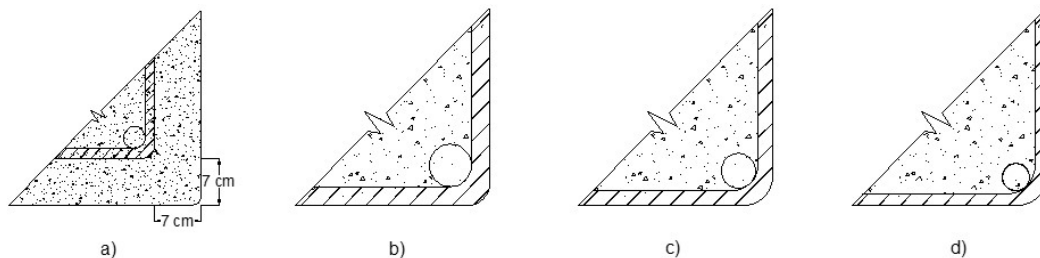


Fig. 5– Used degradation process: a) without damage, b) light damage (cover loss), c) moderate damage (decrease rebar area by corrosion) and d) severe damage (mayor area decrease).

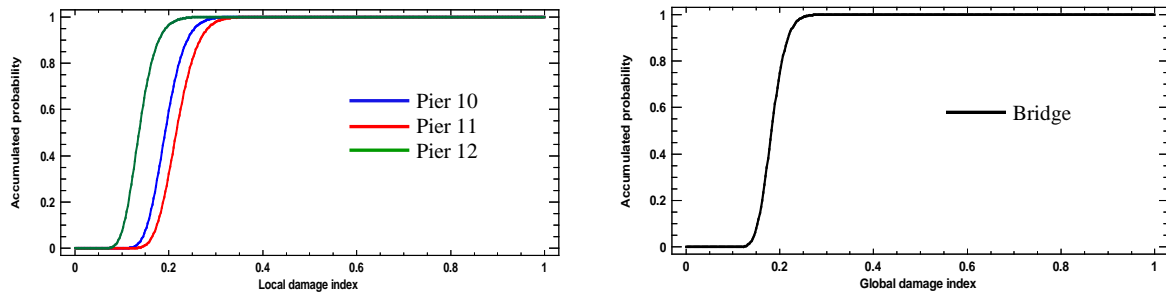


Fig. 6– Fragility curves for piers (left) and the bridge (right) for the first seismic scenario. Light damage on pier 12

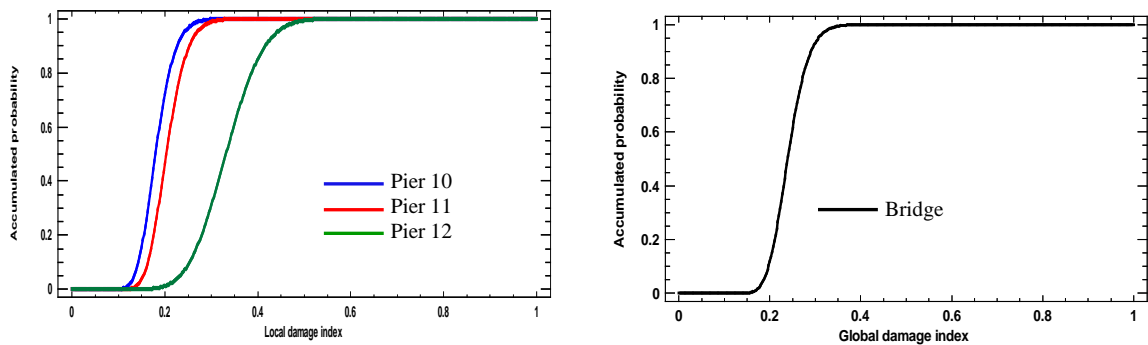


Figure 7– Fragility curves for piers (left) and the bridge (right) for the first seismic scenario. Moderate damage on pier 12

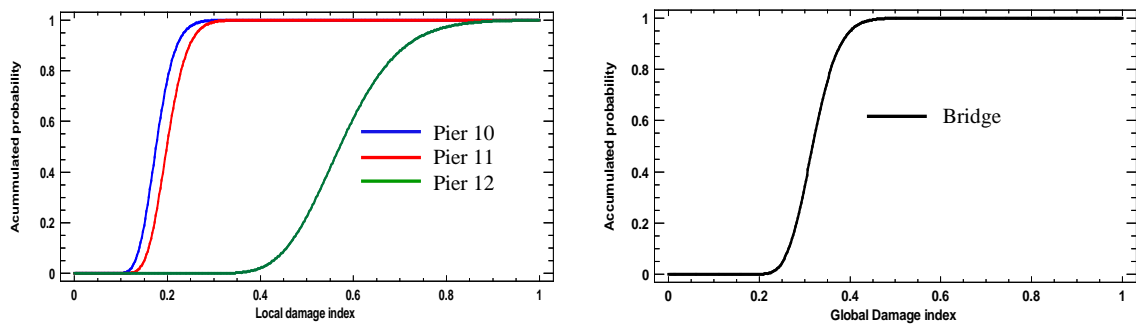


Figure 8– Fragility curves for piers (left) and the bridge (right) for the first seismic scenario. Severe damage on pier 12

In Figure 9 it is observed a comparison of the fragility curves of pier 12, left, and the bridge, right, for different degradations assumed in pier 12 (from not damage to severe damage) for first seismic scenario. A light damage produces a minimum movement to the left of the fragility curves, but moderate and severe damage move this curve to the right, especially for severe damage.



## 2.4 Nonlinear analyses of the rehabilitate bridge

Steel jackets are a retrofit strategy recommended to increase the volumetric ratio of transverse reinforcement, to increase the ultimate compression strain or to increase passive confinement and allow for a larger rotation capacity of columns. After adding some jacket, the columns will be stiffer, and the displacement demand along with the plastic rotation demands are expected to decrease (Shafieezadeh *et al.*, 2009). For circular columns, two half welded shells of steel plate rolled with a radius larger than the original transversal section are collocated over the area to be retrofitted, providing a continuous tube with a small gap of cement grout around the column. For rectangular columns, an elliptical jacket is recommended to proportionate a continuous confining action similar to the circular column. A procedure of column retrofit design with steel jackets can be consulted in Prietley *et al.* (1996). This procedure is based on confinement for flexural ductility enhancement, confinement for flexural integrity of column lap splices, shear resistance enhancement, or stiffness considerations, for circular columns or rectangular columns with an elliptical jacket.

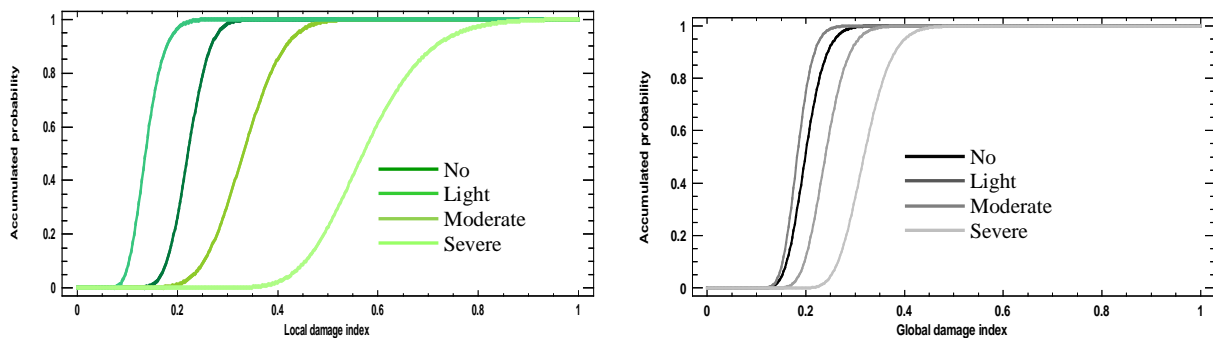


Figure 9– Fragility curves for pier 12 (left) and the bridge (right) for the first seismic scenario. Different damage in pier 12

The concrete jacketing is one of the techniques required reinforcing steel; as an outer layer of steel reinforcement. This technique tends to increase the ability of the section to compression, tension and shear. In addition, this rehabilitation technique is recommended to circular elements, because they lack of corners where stresses are concentrated. For other geometry of transversal section, it requires more careful analysis for the concentration and distribution of reinforcing steel in these areas.

In the nonlinear analysis of original and damaged bridge, moment-curvature and interaction diagrams are defined with SAP 2000 program, using USER DESIGN option. For retrofitted piers, SAP program was not used, because this code considers a perfect adherence between the original material and the new one. In this case, moment-curvature diagrams were performed using OpenSees (Mazzoni *et al.*, 2006) in order to determine the capacities of a rectangular reinforced concrete section covered with steel plates. Rectangular patches were used to generate the cross-section: reinforced concrete unconfined region, reinforced concrete confined region, reinforcing steel bars and cover steel plates. Patches were discretized into fibers with quadrilateral shapes and a straight line of fibers for reinforced steel bars and four integration points per element. The Chang and Mander's concrete model (Concrete 07) with simplified unloading and reloading curves for unconfined and confined regions, was considered. Also, for reinforcing steel bars was used the *Uniaxial bilinear steel material* object, with kinematic hardening and optional isotropic hardening described by a non-linear evolution equation; while for the steel plates fibers was applied the *Uniaxial Giuffre-Menegotto-Pinto steel material* (Steel 02), with kinematic and isotropic hardening.

For Motín de Oro 12 pier, the two half welded shells of steel plate procedure cannot be used because the piers have wall transversal section. Then, four welded plates were proposed, with a thickness of a compact section that produces a similar fragility curve of the original structure. Specifically, in pier 12 steel jackets were



considered with plates of a thickness of 0.64 cm (1/4 in), the minor thickness for a compact section. For light and moderate damage and this retrofit, the local damage index is null for the majority of the 300 variations. Then fragility curves were not elaborated. For pier 12 with a severe damage, a plate with a thickness of 0.79 cm (5/16 in) yields to a fragility curves that are shown in Figure 10. In this figure, compared with Figure 4, fragility curves for pier 10 and 11 are moved to the right of the original curve, but fragility curve for pier 12 was moved to the left. Now, the probability of a damage larger than a moderate condition,  $P[Damage > 0.2/SS1]$ , was a certain event for piers 10 and 11, but a null event for pier 12. For the whole bridge, this probability is over 0.95.

For concrete jackets, the commercial resins were applied to justify the homogeneity between new and old concrete. Then, in OpenSees and SAP models were discretized the old element, resins and concrete jacket to the correct definition of interaction and moment-curvature diagrams. For light damage, a layer of concrete 5 cm thickness is added, and to give confinement, conventional wire mesh 6"x 6" at the center of the layer was used; the fragility curves were not obtained due to little damage presented. For moderate and severe damage, bars of #3 was used, the same spacing of the mesh, since the increase of steel area is not large, and the concrete layer were increased to 8 cm, trying to represent the interaction diagram of the no damaged element, for the original condition of the pier. The fragility curves for concrete jackets and seismic severe damage are shown in Figure 10. For the random variables of the concrete jacket, the same probabilistic properties, but with a new generation of random numbers, were used.

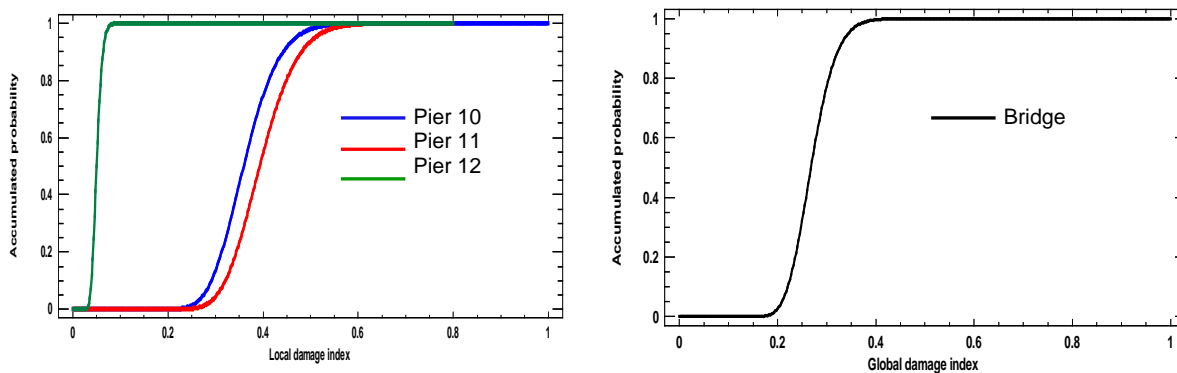


Figure 10– Fragility curves for piers (left) and the bridge (right) for the first seismic scenario. Severe damage on pier 12 with steel jackets

In Figure 11, there is a comparison of the fragility curves obtained for pier 12 for different conditions and for the first seismic scenario. It can be observed the fragility curves for the original structure, the systems when the pier 12 have light, moderate and severe damage and for the structure with severe damage reinforced with steel, concrete and fiber jackets.

As it is observed in Figure 11, original and light damage options have similar fragility curves. When more damage is considered in pier 12, the damage probability is greater and its fragility curves approaches to damage certain event. When the pier is repaired with jackets, the fragility curves move to the left, producing minor probability of exceeds certain damage. In this case, the steel jacket option has the less probability to exceed certain damage, although the only comparison between the three jacket options is the design procedure. Concrete jackets have the minor cost and fiber jacket the greater.

Table 2 shows the probabilities  $P[Damage > 0.2/SS1]$  for all the analyzed options for the three piers and for the bridge. In can be observed that the probability of a reparable damage changes for this condition. For example, when the pier 12 is repaired with concrete jackets, when severe damage is presented, the bridge has a weight mean probability of  $P[Damage > 0.2/SS1]=0.60$ , minor than the certain event when pier has severe damage.

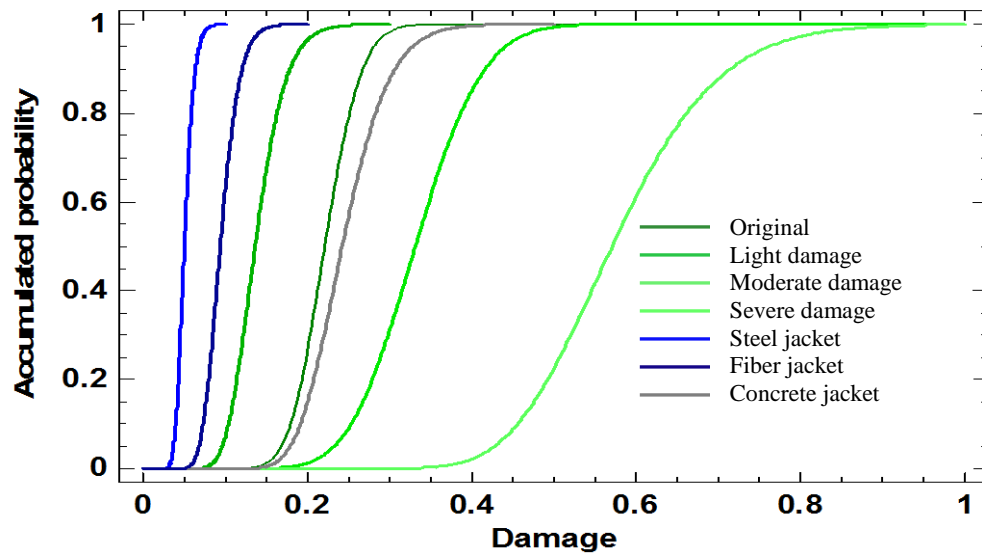


Figure 11– Comparison of fragility curves for pier 12 and the first seismic scenario. Condition of severe damage on pier 12 when different rehabilitation techniques were used

Table 2 – Probabilities  $P[Damage > 0.2/SS1]$  for the analyzed options

Case	Pier 10	Pier 11	Pier 12	Bridge
Original	0.26	0.50	0.75	0.45
Light damage	0.40	0.70	0.10	0.22
Moderate damage	0.25	0.50	0.98	0.90
Severe damage	0.25	0.52	1.00	0.95
Steel jackets, severe damage	1.00	1.00	0.00	0.95
Concrete jackets, light damage	0.35	0.62	0.15	0.30
Concrete jackets, moderate damage	0.30	0.63	0.05	0.10
Concrete jackets, severe damage	0.20	0.42	0.85	0.60
Fibber jackets, severe damage	1.00	1.00	0.02	1.00

#### 4. Final comments

The evaluation of the efficiency of some jacketing techniques to repair bridge pier elements with different damage conditions was evaluated in this paper. The efficiency is defined in function of the change of the probability to exceed certain damage level, through fragility curves. So, a bridge is studied considering its initial condition, without damage, and with light, moderate and severe damage of the pier more susceptible to seismic damage (pier 12), modeled by reduction of its dimensions and properties, conform experimental evaluations available in literature. For these options, fragility curves were defined considering uncertain in mechanical properties of materials and artificial records for seismic scenarios defined in the bridge location, the Pacific Coast of México. For every damage condition, steel, concrete and fibber jackets were designed for the damaged pier and again, fragility curves were defined for all piers and for the bridge, using a weight mean damage. The comparison of the obtained fragility curves defines some comments and conclusions:



- When pier 12 has light damage, it only loses the concrete cover. With moderate and severe damage the reinforcing steel and part of the confined concrete were degraded.
- For light damage on pier 12, the minimal compact section was used for steel jackets and the minimum thickness of concrete and fiber jackets. The majority part of the probabilistic variations for steel and fiber jackets indicate not damaged pier 12, so fragility curves were not elaborated. With concrete jackets, most of the damage of pier 12 is minimal. For this last case, the replacement of the concrete cover will be sufficient, without including some type of jackets.
- For model with moderate damage, Steel and fiber jackets produce a small number of variations with damage in pier 12.
- For models with severe damage, steel, concrete and fiber thickness are greater than minimum values. For these cases, the original and concrete jackets fragility curves are similar. Fragility curves for steel and fiber jackets are to the left of the original curve. With steel and fiber jackets more stiffness and capacity to shear and flexion moment were obtained. The three jackets options proportionate good results, in terms to reduce the probability damage of degraded elements; then cost and fabrication process could be considered as decision aspects for which repair technique would be used.
- For conditions where fragility curves were not possible to obtain, mean damage values were analyzed. Mean values for systems repaired with jackets are greater for piers not repaired and minor for pier 12.
- To repair only part of columns were not considered. When the most susceptible element (pier 12) has moderate or severe damage, other elements have certain probability of damage, however it was not considered.
- Fragility curves for other seismic scenarios were also evaluated, but not presented by space limitations. For the four seismic scenario minimum damage was defined in the bridge. For other seismic scenarios similar conclusions were obtained.
- Fragility curves, and variables that describe the probabilistic behavior of elements of bridges, could be used as another instrument to indicate the damage variation, so they can be used as decision tools to define reinforced options.

## 5. Acknowledgements

This investigation was partially supported by the Universidad Autónoma Metropolitana (UAM, through an internal project) and the PRODEP organization, of the Mexican Public Education Secretary, by the formation of research networks program. Second author express his acknowledgements to CONACYT organization for the grant used to finish his master degree. Thanks to Professors Edgar Tapia y David De León for the participation and comments during the development of this work.

## 6. References

- [1] Car, A J (2004): Ruaumoko 3D. Inelastic dynamic analyses, Civil Engineering Department, University of Canterbury.
- [2] Choi, E, DesRoches R and Nielson B (2004): Seismic fragility of typical bridges in moderate seismic zones": *Engineering Structures*, 26, 187-199.
- [3] Gómez, C and Soria I (2014): Vulnerability evaluation of common simple supported bridges", *10th National Conference on Earthquake Engineering*, Paper 687, Alaska, USA.
- [4] Karim K R and Yamazaki F (2000): Comparison of empirical and analytical fragility curves for RC bridges in Japan, 8th ASCE Special Conference on Probabilistic Mechanics and Structural Reliability.
- [5] Liao W and Loh C (2004): Preliminary study on the fragility curves for highway bridges in Taiwan, *Journal of the Chinese Institute of Engineering*, 27 (3), 367-375.



- [6] Mackie K R and Nielson B G (2009): Uncertainty quantification in analytical bridge fragility curves, Lifeline Earthquake in a Multi-hazard Environment, ASCE, 148.206.91.180.
- [7] Mazzoni S, McKenna F, Scott M, and Fences G (2006): Open system for earthquake engineering simulation, user command-language manual, *Report NEES grid-TR 2004-21*. Pacific Earthquake Engineering Research, University of California, Berkeley, CA.
- [8] Mohsebn M (2012): Dynamic vulnerability assessment of highway and railway bridges. Thesis of Doctor of Philosophy, University of Nebraska, Lincoln, States Unites.
- [9] Nasseradi K, Ghafory-Ashtiany M, Eshghi S and Zolfaghari M R (2009): Developing seismic fragility functions of structures by stochastic approach”. *Asian Journal of Civil Engineering*, 10 (2), 183-200.
- [10] Nielson B G and DesRoches R (2007): Analytical seismic fragility curves for typical bridges in the central and Southeastern United States, *Earthquake Spectra*, 23 (3), 615-633.
- [11] Olmos B, Jara J M, Gómez, C and Jara M (2014): Seismic response of bridges with a pier substructure reinforced with steel jacketing. *5as Jornadas Portuguesas de Engenharia de Estruturas, JPPE*, Paper 136, Portugal.
- [12] Padgett J E and DesRoches R (2008): Methodology for the development of analytical fragility curves for retrofitted bridges, *Earthquake Engineering and Structural Dynamics*, (37), 1157-1174. DOI:10.1002/eqe.801m.
- [13] Park Y J and Ang A H (1985): Mechanistic seismic damage model for reinforced concrete, *Journal of Structural Division (ASCE)*, 111 (4) 722-739.
- [14] Posada B (1994): La degradación del concreto armado. *Revista Universidad EAFIT, Colombia*. 30 (93), 16-20.
- [15] Priestley M J and Park Y J (1989): Strength and ductility of concrete bridge columns under seismic loading, *ACI Structural Journal*, Title No. 84-S8.
- [16] Priestley M J, Seibel F and Calve G M (1996): *Seismic design and retrofit of bridges*, John Wiley & Sons, New York, USA.
- [17] SAP2000, Advanced 15.1 (2008): Integrated solution for structural analyses and design, Computer and Structures INC.
- [18] Shafieezadeh A, Hu W, Erduran E and Ryan K L (2009): Seismic vulnerability assessment and retrofit recommendations for state highway bridges: case studies. *Report UT-0908*. Utah Department of Transportation Research Division.
- [19] Zhang J Y, Huo S, Brandenberg J and Kashighadi P. (2008): Effects of structural characterization on fragility functions of bridges subjected to seismic shaking and lateral spreading, *Earthquake Engineering and Engineering Vibrations*, 7 (4), 369-382, DOI: 10.1007/s 1803.008.1009-2.